

EXAFS Energy Shift and Structural Parameters

Shelly D. Kelly and Bruce Ravel

Argonne National Laboratory, 9700 South Cass Avenue, Argonne, IL 60439

Abstract. In EXAFS analysis, the energy shift parameter is used to align the theoretical calculated spectrum to the energy grid of the measured spectrum. Unrealistically large energy shift values, sometimes in excess of 20 eV, are at times published in research articles. We therefore see the need for a concise discussion of the EXAFS energy shift parameter. This paper is intended as a learning tool for the proper alignment of theory to measured EXAFS spectra and proper interpretation of the energy shift parameter.

Keywords: EXAFS, Energy Shift

PACS: 87.64.Fb

INTRODUCTION

In EXAFS analysis, the energy shift parameter, ΔE_0 , is used to align the theoretical calculated spectrum to the energy grid of the measured spectrum. This parameter is rarely emphasized in research articles and is often not reported at all. Unrealistically large ΔE_0 values, sometimes in excess of 20 eV, are at times reported. We surveyed 14 manuscripts containing tables of EXAFS results and found 4 reported ΔE_0 values of < 10 eV and 3 ΔE_0 values > 10 eV; 7 papers did not report ΔE_0 values [1-14]. We, therefore see the need for a concise discussion of ΔE_0 . Here we explain why a small energy shift is generally desirable and demonstrate how to minimize the value for ΔE_0 by using two examples. In the first example, a synthetic EXAFS spectrum from scorodite (As-Fe) generated and modeled with FEFF and a large ΔE_0 value demonstrates that the path length variable is highly correlated to ΔE_0 . In the second example, we attempt to show how a large ΔE_0 value can be obtained with seemingly reasonable EXAFS parameters. In this example, an edge energy position, E_0 , is chosen well below the rising edge of the measured AsS spectrum at the stage of background removal, and the resulting EXAFS spectrum is analyzed. We demonstrate the proper steps needed to align the measured spectra to the theoretical spectra and compare the resulting structural parameters for the shifted spectra. This paper is intended as a learning tool for the proper alignment of theory to measured EXAFS spectra and the proper interpretation of ΔE_0 values.

MATERIALS AND METHODS

Arsenic k -edge EXAFS spectra from AsS (realgar) at 10K were taken from the standards database [15]. The data were collected at SSRL beamline 2-3. The sample was prepared as a powder on five layers of tape. The incident and transmission ionization chambers were filled with N_2 and Ar, respectively. The vertical Si(111) monochromator slits had an opening of 0.6 mm. The second crystal was detuned by 75% to reduce the harmonic x-ray intensity.

Three EXAFS spectra were aligned and then averaged. The background was removed by using Athena [16], an interface to IFEFFIT [17]. The background parameter Rbkg was set to 1.0 Å. The FEFF7 [18] calculation is based on the crystal structure of realgar for AsS and scorodite for an As-Fe path ($R = 3.3$ Å).

The theoretical As-Fe scattering path was modeled with the same theoretical path but with an imposed ΔE_0 of 20 eV. The Fourier transform (FT) of the data was derived at 4.0–14.5 Å⁻¹ and modeled at 2.2–3.4 Å.

The AsS EXAFS spectrum, $\chi(k)$, was produced with E_0 on the rising part of the absorption edge, as determined by default within Athena, with a -10-eV shift from this value and again with a -20-eV shift. To obtain reasonable background subtraction, the spline region was defined to include the same region of the spectrum. This was accomplished by using minimum k values in the background spline of 0.5, 2.1, and 2.6 Å⁻¹ for the 0-eV-, -10-eV-, and -20-eV-shifted spectra, respectively.

TABLE 1. EXAFS results for As-Fe theoretical spectra.

Model	CN·S ₀ ²	ΔR (Å)	σ ² (10 ⁻³ Å ²)	ΔE ₀ (eV)
One-shell model				
As-Fe	0.7(1)	-0.18(1)	5(1)	33(2)
Two-shell model				
As-Fe1	1.6(4)	-0.15(1)	9(1)	35(2)
As-Fe2	0.8(4)	0.09(1)		
Theoretical As-Fe data				
As-Fe	1.0	0	5	0

The EXAFS model for AsS contains two scattering paths for the photoelectron. The first path is a single scattering (SS) path from the two S atoms ($R = 2.23$ Å). The second SS path is from one As atom ($R = 2.58$ Å). The model includes independent ΔR and σ^2 values for the two paths. One energy shift, ΔE_0 , and one amplitude reduction factor, S_0^2 , were determined in the model fit to the spectrum.

RESULTS AND CONCLUSIONS

TABLE 2. EXAFS results for AsS with different choices for E_0 and XRD distances.

Data	CN and Path	S ₀ ²	R (Å)	σ ² (10 ⁻³ Å ²)	ΔE ₀ (eV)
0 eV	2 As-S	1.06 (6)	2.27(1)	2.0(4)	6(1)
	1 As-As		2.54(1)	8(2)	
-10 eV	2 As-S	1.01(6)	2.26(1)	1.6(5)	15(1)
	1 As-As		2.53(1)	7(2)	
-20 eV	2 As-S	0.99(6)	2.26(1)	1.5(5)	25(1)
	1 As-As		2.53(1)	7(1)	
Using theory	2 As-S	1.10(6)	2.26(1)	2.2(5)	1.9(6)
	1 As-As		2.54(1)	9(2)	
XRD	2 As-S		2.23		
	1 As-As		2.58		

To illustrate a model fit with a large mismatch between the measured and theoretical spectra, we calculated the As-Fe path ($R = 3.3$ Å) from scorodite. The theoretical data were produced with the EXAFS parameters listed in Table 1. Two theoretical models (one with a single As-Fe path and another with two As-Fe paths) were constructed to reproduce the theoretical data with an initial ΔE_0 value of 20 eV. The theoretical EXAFS data and these model fits are in Figure 1, and the EXAFS parameters are in Table 1. For both models, the 20-eV shift value was unstable; the resulting best-fit value for ΔE_0 is close to 34 eV. With this energy shift, the models accurately describe the theoretical data, but they give erroneous values of 0.7–1.6 for CN and of -0.18 to 0.09 Å for ΔR , as compared to the theoretical data of CN = 1.0 and $\Delta R =$

0.0 Å. These models show that one or two signals with large energy shift values can be used to describe an unshifted spectrum. In many applications of EXAFS, the numbers of coordination shells are not known, and either of these models could be presented by mistake. Therefore, it is best to minimize ΔE_0 and accurately align the edge energy E_0 with the theoretical spectra as described below. First we explore the possibility of a large energy shift for both the theoretical and measured spectra, in an attempt to reproduce similar energy shift values with seemingly reasonable structural parameters reported in the literature.

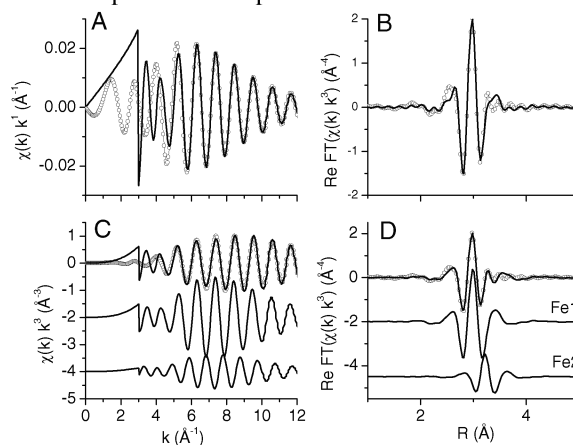


FIGURE 1. Comparison of unshifted theory (symbols) and theory with a 20-eV shift (line) of the $\chi(k)$ spectra (A and C) and the real part of the FT (B and D). A and B show the best match for a single 20-eV-shifted model. C and D show the best fit for two 20-eV-shifted models. Each component of the model is shown below the total.

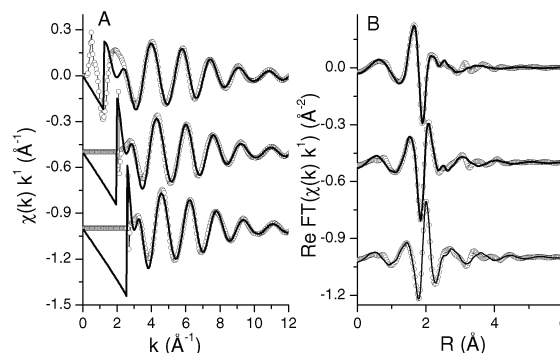


FIGURE 2. Comparison of EXAFS data (symbols) and theory (line) for the $\chi(k)$ spectrum (A) and the real part of the FT (B). The top, middle, and bottom spectra have E_0 set at the default value, the default value - 10 eV, and the default value - 20 eV.

In many of the EXAFS manuscripts with large ΔE_0 values, the EXAFS parameters for CN, ΔR , and σ^2 seem to describe the standard spectra accurately, where the structural parameters are known. Here we present a method that may give these results, by shifting both the data and the theoretical spectra by

large ΔE_0 values. The reason for choosing the edge energy E_0 away from the rising part of the absorption edge may be monochromator energy values poorly calibrated with the atomic edge energy value for E_0 . The reason could also be noisy data, where the default edge energy in Athena is poorly chosen. The EXAFS spectra generated by choosing E_0 at the default (within Athena) location on the edge, at -10 eV from the default value, and at -20 eV from the default values are compared in Figure 2A. The AsS model described above was optimized to these spectra, as shown in Figure 2, with the best-fit values in Table 2. The best-fit values are very similar for all EXAFS spectra. The ΔE_0 found by the fitting procedure for the 0-eV-shifted spectrum indicates that the original E_0 value on the edge is approximately 6 ± 1 eV from the theoretical value determined by the model. The -10-eV-shifted and the -20-eV-shifted spectra have ΔE_0 values of approximately 10 eV and 20 eV more, respectively, than the 0-eV-shifted spectrum. The similarity in the EXAFS results for the path length R and σ^2 , along with the appropriately shifted ΔE_0 values, shows that a shifted spectrum can be described accurately with a shifted theory. This may be the effect being illustrated in several manuscripts with very large ΔE_0 values but seemingly reasonable fit values.

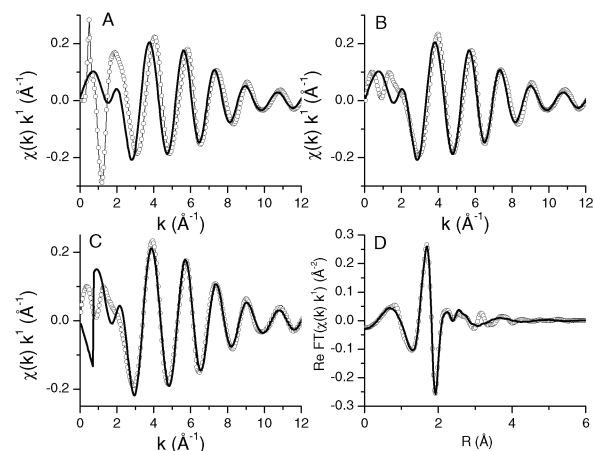


FIGURE 3. Comparison of EXAFS data (symbols) and theory (line). A) Original theory and model fit with ΔE_0 of zero. B) Theory from (A), used to find E_0 (the edge energy) and produce an EXAFS spectrum that is well aligned with the theory. C and D) Final EXAFS data and model fit.

Because large ΔE_0 values are not necessary and could indicate potential problems in the fitting procedure, the edge energy value E_0 should be calibrated to the theoretical spectra, small ΔE_0 values should be obtained when modeling the spectra.

To properly align the EXAFS spectra to the theory, the E_0 value in the background removal step needs to be adjusted. Figure 3A shows the original 0-eV-shifted

spectrum from Figure 2. The theory is shown with the best-fit values for all the EXAFS parameters except for ΔE_0 , which is zero. This unshifted theory is then used in the background removal step to choose the edge energy position accurately. The aligned spectra and the theoretical spectra should cross zero together at low wave numbers, as shown in Figure 3B. The aligned data are modeled with the theory as shown in Figure 3C and 3D. The final EXAFS parameters are shown in Table 2. The small energy shift value of 1.9 ± 0.6 eV indicates that the theory and the measured spectra are well aligned. This procedure will preclude arriving at the erroneous minima found by modeling unshifted data with a shifted model (Table 1).

Acknowledgements: Our work is supported by the ERSD-BER, Office of Science, Department of Energy, under contract W-31-109-Eng-38.

REFERENCES

1. G. Ona-Nguema, G. Morin, F. Juillot et al., *Environmental Science & Technology* **39** (23), 9147 (2005).
2. G. S. Cargill and M. Matsuura, *Journal of Non-Crystalline Solids* **150** (1-3), 347 (1992).
3. A. L. Foster, G. E. Brown, T. N. Tingle et al., *American Mineralogist* **83** (5-6), 553 (1998).
4. A. Puig-Molina, L. P. Nielsen, A. M. Molenbroek et al., *Catalysis Letters* **92** (1-2), 29 (2004).
5. D. Testemale, J. L. Hazemann, G. S. Pokrovski et al., *Journal of Chemical Physics* **121** (18), 8973 (2004).
6. M. C. Teixeira and V. S. T. Ciminelli, *Environmental Science & Technology* **39** (3), 895 (2005).
7. B. T. Beaulieu and K. S. Savage, *Environmental Science & Technology* **39** (10), 3571 (2005).
8. C. Y. Jing, S. Q. Liu, M. Patel et al., *Environmental Science & Technology* **39** (14), 5481 (2005).
9. G. Waychunas, T. Trainor, P. Eng et al., *Analytical and Bioanalytical Chemistry* **383** (1), 12 (2005).
10. S. J. Wasson, W. P. Linak, B. K. Gullett et al., *Environmental Science & Technology* **39** (22), 8865 (2005).
11. S. Thorat, J. Rose, J. M. Garnier et al., *Environmental Science & Technology* **39** (24), 9478 (2005).
12. B. Cances, F. Juillot, G. Morin et al., *Environmental Science & Technology* **39** (24), 9398 (2005).
13. D. G. Beak, N. T. Basta, K. G. Scheckel et al., *Environmental Science & Technology* **40** (4), 1364 (2006).
14. M. Pena, X. G. Meng, G. P. Korfiatis et al., *Environmental Science & Technology* **40** (4), 1257 (2006).
15. M. Newville, S. A. Carroll, P. A. O'Day et al., *Journal of Synchrotron Radiation* **6**, 276 (1999).
16. B. Ravel and M. Newville, *J. Synch. Rad.* **12** (4), 537 (2005).
17. M. Newville, *J. Synch. Rad.* **8**, 322 (2001).
18. S. I. Zabinsky, J. J. Rehr, A. Ankudinov et al., *Phys. Rev. B* **52** (4), 2995 (1995).